BBD Memo #033

Massachusetts Institute of Technology
Haystack Observatory
WESTFORD, MASSACHUSETTS 01886

DATE 07/15/2009

To: Broadband Development Group

From: C. J. Beaudoin

Subject: Holographic Processing and Considerations for VLBI2010 Antenna Diagnostics

Holographic Processing

Consider the antenna aperture shown in figure 1, radiating (or receiving by reciprocity) at frequency *f*, and having a singularly (x) polarized electric field distribution given by $\overline{E}_x\left(x_{apt}, y_{apt}\right)$; the unknown aperture distribution. Given samples of the far-field receive pattern of $\overline{E}_x\left(x_{apt}, y_{apt}\right)$, the aperture distribution function can be reconstructed by the following formulation:

$$\overline{E}_x\left(x_{apt}, y_{apt}\right) = \iint_{\theta,\phi} \overline{E}_x^{ff}\left(F_x, F_y\right) e^{j\left(x_{apt}F_x + y_{apt}F_y\right)} dF_x dF_y \tag{1a}$$

$$F_x = \frac{2\pi f}{c}\sin(\theta)\cos(\phi) \tag{1b}$$

$$F_y = \frac{2\pi f}{c}\sin(\theta)\sin(\phi) \tag{1c}$$

Where θ, ϕ are as depicted in figure 1 and define the location of the far-field source relative to the aperture. The integration of equation 1a is performed over the range of θ and ϕ for which there is knowledge of the far-field radiation pattern $\overline{E}_x^{ff}$. Equation 1a relates the aperture distribution function to the two-dimensional Fourier transform of the far-field pattern; normalization constants have been suppressed. Equations 1b and 1c are formatting equations which indicate where the far-field samples must be located in Fourier space in order to successfully reconstruct the aperture distribution using the Fourier-based method. A benefit of incorporating this method is that one can employ properties of the multi-dimensional Fourier transform when analyzing imagery generated from such holographic processing.

Data collected for holographic processing are done so by scanning the antenna under test (AUT) through a source at some azimuth and elevation angle in the antenna coordinate system which is fixed relative to the physical ground plane. The angles θ and ϕ, on the other hand, are defined in the aperture coordinate system and change as a

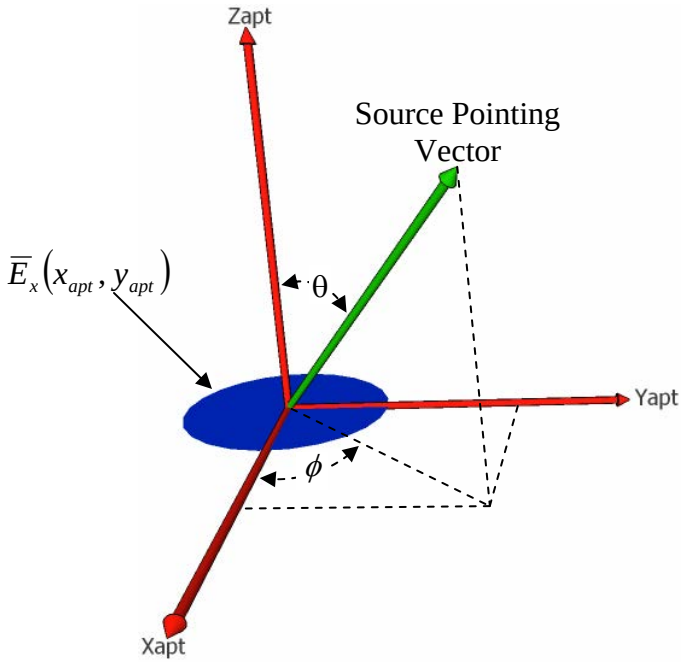

Figure 1: Geometry depicting the antenna aperture in the aperture coordinate System.

function of antenna pointing. As such, the source pointing vector defined by θ and ϕ must be related to the antenna azimuth and elevation pointing angles in order to give them meaning for the application at hand. Figure 2 displays this relationship which is defined by the following transformation:

$$\begin{bmatrix} F_x \\ F_y \\ F_z \end{bmatrix} = \frac{2\pi f}{c} \begin{bmatrix} -\sin(\phi_s) & \cos(\phi_s) & 0 \\ -\sin(\psi_s)\cos(\phi_s) & -\sin(\psi_s)\sin(\phi_s) & \cos(\psi_s) \\ \cos(\psi_s)\cos(\phi_s) & \cos(\psi_s)\sin(\phi_s) & \sin(\psi_s) \end{bmatrix} P_{ant} \tag{2}$$

Here, P_{ant} is the antenna pointing unit vector in the antenna coordinate system and ψ_s and ϕ_s are the elevation and azimuth pointing angles, respectively, to the source being used to measure the far-field pattern. Based on figure 2 and equation 2, one will observe that at $\psi_s = \phi_s = 0°$, the x_{ant} axis coincides with the z_{apt} axis (source pointing vector) of the aperture system. In figure 3, the source pointing vector (green vector in figure 2) coincides with z_{apt}.

The significance of the transformation described by equation 2 is that it describes how say a uniform azimuth and elevation sampling grid in the antenna system is deformed into a nonuniform sample grid in the Fourier space. As an example, assume that a holographic data collection is performed whereby a sampling grid is constructed using 5° steps spanning 40° in azimuth and elevation and the source is located at 45° elevation and 0° azimuth. Figure 3 displays the F_x,F_y spatial frequency mapping of the samples given the specified antenna raster scan.

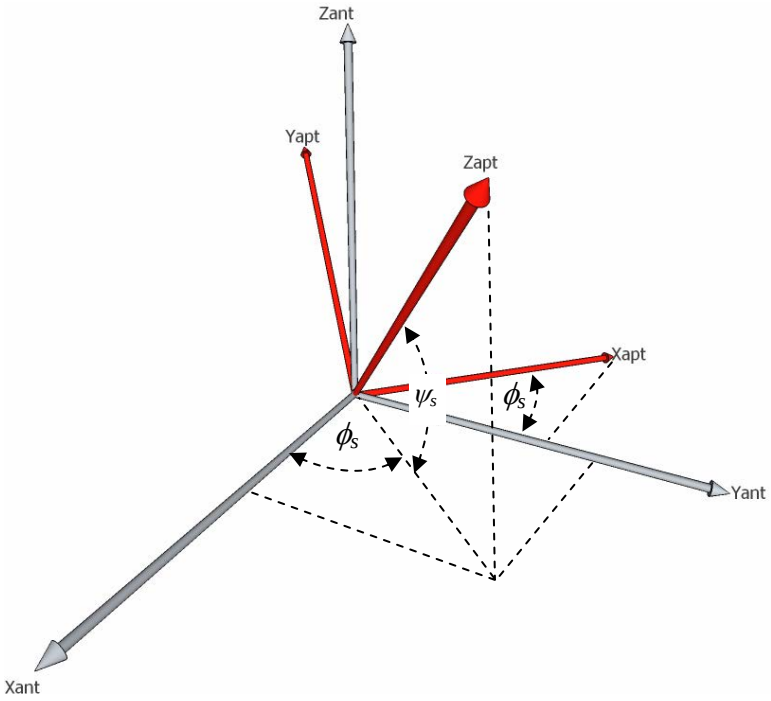

Figure 2: Relationship of antenna (grey) and aperture (red) coordinate systems through the source azimuth (ϕ_p) and elevation (ψ_p) angles when the antenna is pointed on-source.

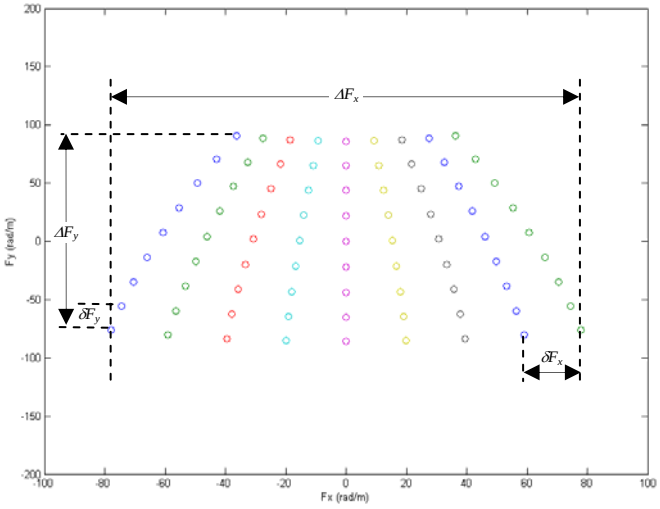

Figure 3: Example mapping of nonuniformly distributed Fourier space samples obtained from uniform sampling in antenna azimuth and elevation.

In order to reconstruct a hologram given a sample mapping such as that shown in Figure 3, two methods may be incorporated. The first method, which is technically straightforward yet computationally intensive, explicitly evaluates equation 1. This amounts to calculating a discrete Fourier transform which requires that a 2D complex weighting and summing of $\overline{E}_x^{ff}$ be performed for each pixel evaluated in the hologram. A more efficient and widely used approach is to resample the nonuniform Fourier space grid to one that is uniform and then employ a 2D FFT routine. In the interest of development time, the first method has been implemented in MATLAB code. If processor speed become an issue using this method, a sinc interpolant can be developed to speed up the calculations by implementing the second method.

Resolution of a holographic image reconstruction is an important parameter to consider when diagnosing the performance of an antenna. Since the Fourier spatial frequency counterparts to x_{apt} and y_{apt} are F_x and F_y, respectively, the x_{apt},y_{apt} holographic image resolutions, δx and δy, respectively, are inversely proportional to the spatial frequency span of the data in each dimensions. Formally expressed:

$$\delta x = \frac{2\pi}{\Delta F_x} \tag{3a}$$

$$\delta y = \frac{2\pi}{\Delta F_y} \tag{3b}$$

where ΔF_x and ΔF_y are the span of the data in the F_x and F_y dimensions, respectively. In regards to a spatial frequency mapping, ΔF_x and ΔF_y are taken as shown in figure 3.

Conversely to image resolution, the unambiguous size of the hologram that can be reconstructed is dependant on the spacing of the samples in the Fourier space which is also depicted in figure 3. The largest spacing of the samples in the F_x and F_y dimensions is used to determine the unambiguous image size in the x_{apt} and y_{apt} dimensions:

$$\Delta x = \frac{2\pi}{\delta F_x} \tag{4a}$$

$$\Delta y = \frac{2\pi}{\delta F_y} \tag{4b}$$

Here Δx and Δy are the unambiguous size of the image in the x_{apt} and y_{apt} dimensions and δF_x and δF_y are the maximum F_x and F_y sample spacings, respectively.

Lastly, the image phase of a holographic reconstruction can be used to infer information about height relative to the aperture plane. This is done using the following relation:

$$z_p = \frac{c}{2\pi f}\Phi_p \tag{5}$$

where Φ_p is the phase of any given pixel in the image and z_p is the inferred height of that particular pixel out of the aperture plane. This technique is only applicable to those pixels which have appreciable amplitude in the hologram.

Processor Performance with Simulated Data

As a demonstration of the processor's performance, a simulated holographic data set was created by modeling the far-field pattern of a 5 meter circular aperture possessing a 2m circular distortion:

$$\overline{E}_x^{ff} = \frac{J_1(2.5k\sin(\theta))}{2.5k\sin(\theta)} + \left(\frac{2}{5}\right)^2 \frac{J_1(k\sin(\theta))}{k\sin(\theta)} e^{jk\sin(\theta)(\cos(\phi)+\sin(\phi))}\left(0.5e^{j(0.010)k\cos(\theta)} - 1\right) \quad (6)$$

where θ and ϕ are as defined in figure 1 and J_1 is the first-order Bessel function of the first kind. In the model described by equation 6, the distortion is offset from the center of the aperture by 1 meter in x_{apt} and y_{apt}, possesses one half the field amplitude of the rest of the aperture, and is displaced 10 mm out of the aperture plane. The data were calculated over elevation and azimuth spans of 10 and 13.25°, respectively, with the source located at 45° elevation angle and 0° azimuth angle. For this particular collection, $\delta x = \delta y = 0.14$ m. Figure 4 displays the magnitude and height profile of the aperture distribution as reconstructed by holographic processing of the simulated far-field data. In observing figure 4, one will observe that the circular shape and relative intensities of the aperture and the distorted area are preserved in the reconstruction. Furthermore, the processor faithfully reproduces the height profile of the radiating aperture relative to the x_{apt},y_{apt} plane.

Considerations in Measuring Far-Field Data

Up to this point, the assumption was made that samples of the test antenna's far-field pattern were available. Also, the development of the holographic processor in the previous section was done so for a single frequency signal. That being said, the phase and magnitude of the far-field samples are obtained by cross-correlating the signal received by the reference antenna (fixed pointing on the source) and that by the AUT (scanned through the source). In accordance with the development of the previous section, the far-field measurement is then the magnitude and phase of the cross-power spectrum (CPS) at a single frequency. Though consistent with the processor development, using only one frequency from the CPS is unsatisfactory because the majority of the data is discarded and SNR is lost. However, if the reciprocal bandwidth of the signals used to generate the cross-correlation function (CCF) is sufficiently large with respect to time delay variations across the aperture (due to antenna imperfections), there will be little phase variation across the CPS and the magnitude/phase of the CCF at it's peak(magnitude) is representative of the complex far-field sample at each point in the raster scan. In practice, the bandwidth of the CCF will probably be 32 MHz, for which the time-delay resolution is 31 ns. The time delay errors across the antenna aperture would have to be extremely gross in order to loose coherence across such a narrow bandwidth. This being the case, it is permissible to use the peaks of the CCFs to provide the complex far-field samples used to reconstruct the hologram.

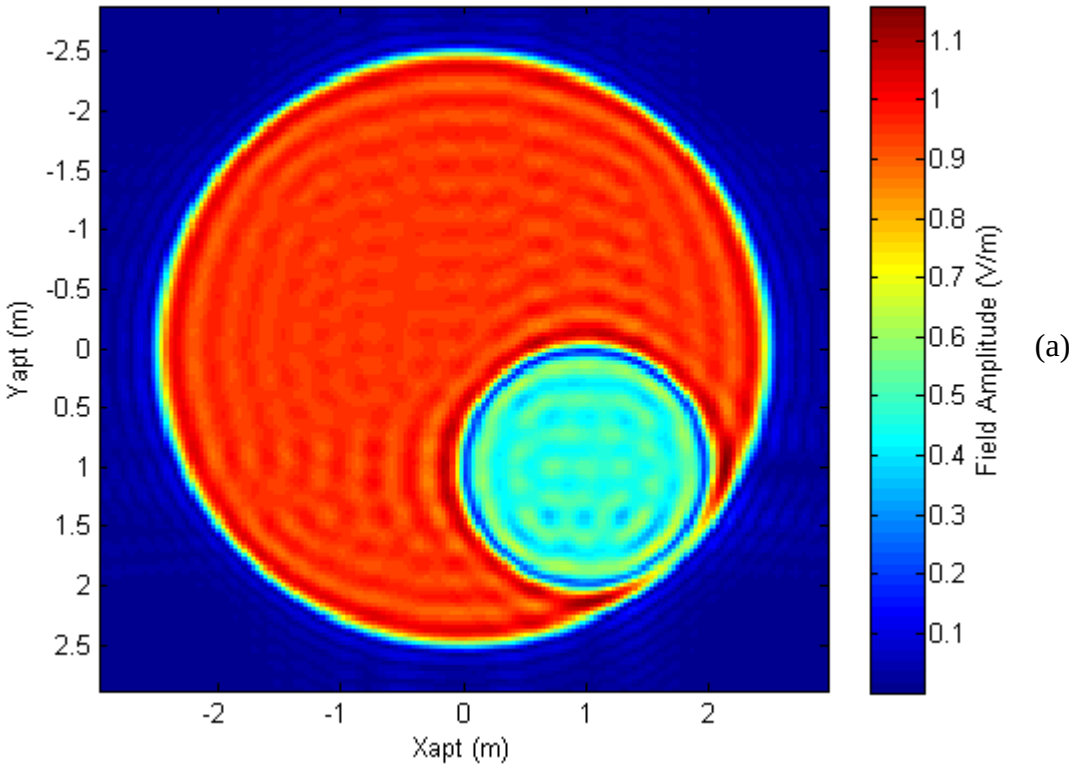

(a)

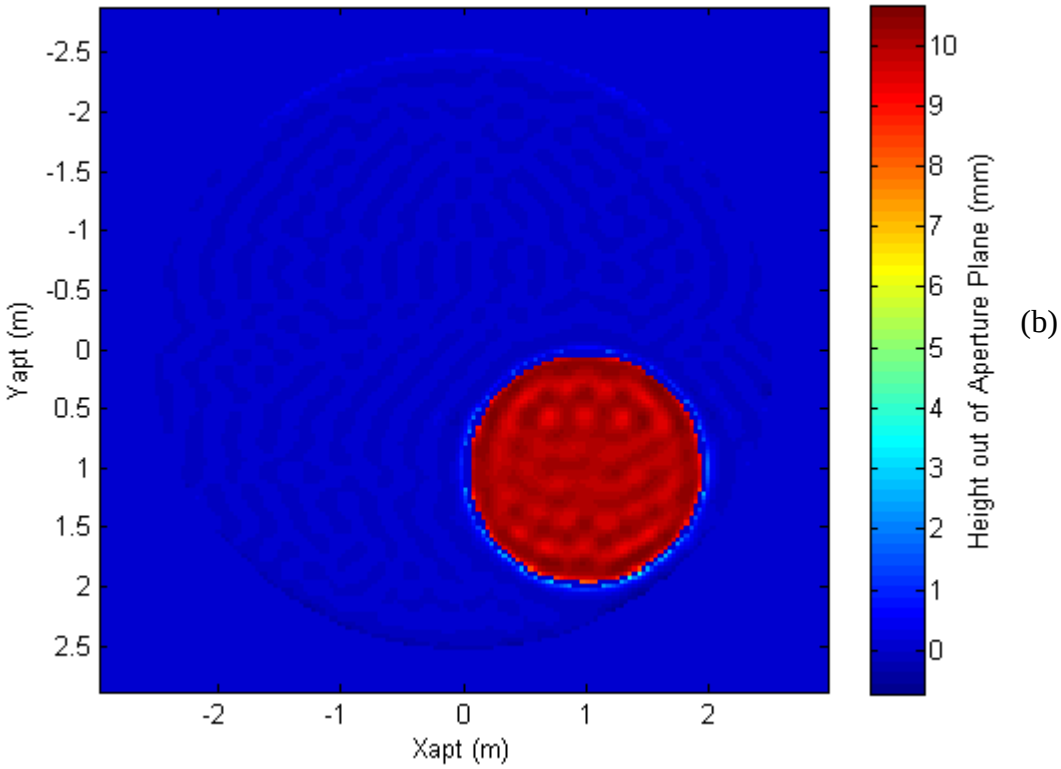

(b)

Figure 4: Holographic reconstruction of data simulating 5m circular aperture with 1m circular distortion. (a) display the magnitude of the electric field in the aperture and (b) displays the height profile of the aperture.

SNR Considerations

It is also worthwhile to evaluate the amount of recording time needed for each scan to achieve a specified maximum rms phase uncertainty (at minimum AUT area when pointed off-source) and hence minimal SNR in the far-field data. Based on rough power measurements of a randomly selected satellite source using one of AEER's VSRTs, the noise power in the source was observed to be 10 dB stronger than that of the LNB. This particular VSRT possessed an LNB with noise temperature of 100K and an 18" aperture with 50% efficiency. Based on the observed power level of the source relative to the LNB noise and the aperture area, in 32 MHz bandwidth the power density available in Haystack parking lot is approximately -82 dBm/m^2.

Based on this power density, assuming a reference antenna possessing 1m aperture with 50% efficiency using a front-end having temperature 100K, the SNR in the reference measurements will be 13.5 dB. Assuming MV3 as the test antenna, that it is operating at 40% efficiency, and that it is pointed +/- 5 deg off-source, the effective area of the antenna when pointed fully off-source, assuming an Airy pattern, is 0.1 m^2. Given that the MV3 antenna temperature is currently 100K and the off-source effective area, the minimum SNR in the AUT observations is expected to be 11.5 dB. Given the single dish SNR in each antenna and assuming 2-bit sampling, the correlation amplitude, ρ_o, is calculated with the following:

$$\rho_o = \frac{1}{1.13} \frac{1}{\sqrt{1 + snr_r^2 + snr_t^2 + snr_r^2 snr_t^2}} \tag{4}$$

where snr_r and snr_t are the single dish signal-to-noise ratio's of the reference and test antennas, respectively. The factor 1/1.13 is the loss as a result of 2-bit sampling. Given the previously calculated single dish SNR quantities, $\rho_o = 0.83$.

Having the correlation amplitude, the total recording time needed to achieve a specified phase uncertainty, σ_ϕ, in the far-field data is given by:

$$T_r = \frac{1}{f_s \left(\sigma_\phi \rho_o\right)^2} \tag{5}$$

where f_s is the data sample rate. With 32 MHz channels, the data sample rate is 64 MS/s and taking σ_ϕ = 1 deg, the recording time needed to achieve the required SNR is 73 us. This record time corresponds to a total sample count of 4672 which is sufficiently small enough to allow the reference/test antenna correlations to be performed on the same computer running the holographic processor.